

# Eigenmode analysis of fishnet metamaterials

Masanobu Iwanaga<sup>1,2</sup>

<sup>1</sup>National Institute for Materials Science (NIMS)

1-1 Namiki, Tsukuba 305-0044, Japan

Fax: + 81-298604679; email: iwanaga.masanobu@nims.go.jp

<sup>2</sup>PRESTO, Japan Science and Technology Agency (JST)

4-1-8 Honcho, Kawaguchi 332-0012, Japan

## Abstract

Eigenmodes in a typical fishnet metamaterial have been clarified based on precise numerical analysis. The lowest mode in energy splits into two branches at in-plane wave vector of  $k \neq 0$ . The lower branch is found to be the mode of in-plane negative group velocity, responsible for negative refraction in fishnet metamaterials.

## 1. Introduction

Fishnet metamaterials (MMs) have attracted great interest as MMs of effective negative refractive index [1]. The concept of effective refractive index comes from the assumption of homogenization of linear optical responses in MMs. From purely structural point of view, fishnet MMs are periodically perforated metal-insulator-metal (MIM) waveguides. It is therefore possible to examine the eigenmodes. To our knowledge, the eigenmodes have not been clarified so far. By analysing the eigenmodes, it is expected to obtain the firm ground characterising the resonances in fishnet MMs and moreover to reveal how the features of the eigenmodes are related to the effective refractive index. In general, eigenmodes provide rich physical insights in plasmonic crystals [2, 3].

In this paper, we focus on to analyse a typical fishnet MM and especially to clarify the lowest eigenmode associated with the effective negative refractive index. In Sec. 2, the concrete structural parameters and optical configuration are shown. In Sec. 3, the dispersion relation of eigenmodes is shown and described by an analytical equation, and the resonant features of electromagnetic (EM) power flow are exhibited, based on precise numerical analyses. In Sec. 4, concise conclusions are given.

## 2. Structure of fishnet MM and optical configuration

Figure 1 shows a fishnet MM of (Au/Al<sub>2</sub>O<sub>3</sub>/Au) on quartz substrate (pale blue). The structural parameters are set to be almost same with the ones in Ref. [1]: the air holes (white) of 400 nm diameter are arrayed in the square lattice of 830 nm periodicity, and the thickness of the three layers in the fishnet MM is 30, 60, and 30 nm. The  $x$  and  $y$  axes are set to be parallel to the square array. In the configuration, the fishnet MM is assumed to periodically spread in the  $xy$  plane and is optically probed by plane wave travelled from air. We here concentrate on this configuration corresponding to experiment. Effective refractive index is usually extracted at the normal incidence, that is, wave vector  $\mathbf{k}_{\text{in}} \parallel \hat{z}$ .

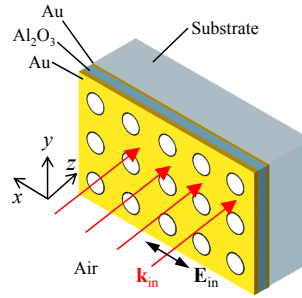


Fig. 1: Fishnet MM, coordinate axes, and optical configuration. Fishnet MM is composed of stacked layers of air-hole array (white). Yellow and dark blue denote Au and  $\text{Al}_2\text{O}_3$ , respectively. Pale blue denotes quartz substrate.

### 3. Features of the lowest eigenmode

Figure 2(a) shows reflectance (R) and transmittance (T) spectra under  $p$  polarization (*i.e.* incident electric field  $\mathbf{E}_{\text{in}}$  parallel to the  $xz$  plane). These spectra were computed with the improved modal Fourier method [4] coupled with scattering matrix method [5]. R spectra of incident angle  $0^\circ$  to  $85^\circ$  are plotted with offset. The permittivity of Au was taken from the literature [6]. The present issue is the lowest mode located at 0.60 eV and  $0^\circ$  incident angle, though the R dip and T enhancement are not prominent compared with the reduced surface plasmon polariton (SPP) at 0.95 eV and  $0^\circ$ , which is consistent with the experimental report [1].

Figure 2(b) shows dispersion plots (closed and open circles, and closed oblique squares) extracted from the R dips in Fig. 2(a). The dispersions are plotted in the plane of normalised  $x$ -parallel in-plane wave vector  $ka/2\pi$  and photon energy in eV, where the  $a$  denotes the periodicity. The red closed circles show the lower branch of the lowest mode under  $p$  polarization. The red open circles present the reduced SPP associated with diffraction. The two decreasing branches are almost linear; on the other hand, the tangents are quite different. We introduce an equation for the dispersion of the lower branch of the lowest mode,

$$\omega = -c(k - 2\pi/a) \sqrt{\frac{d_A}{d_A + (4\pi c/\omega_p) \coth(\omega_p d_M/c)}}, \quad (1)$$

and show it with blue dashed line in Fig. 2(b), where  $d_A$  and  $d_M$  respectively denote the thickness of  $\text{Al}_2\text{O}_3$  and Au layers,  $\omega_p$  is the plasma frequency of Au defined in Drude model [6], and  $c$  is the velocity

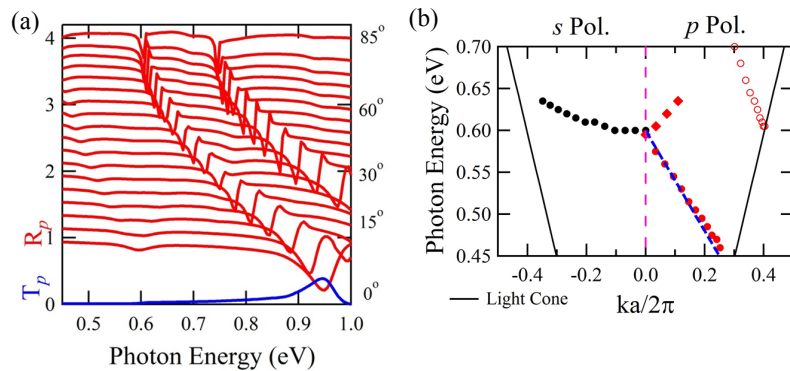


Fig. 2: (a) R spectra (red) displayed with offset from incidence angle  $0^\circ$  to  $85^\circ$  at  $5^\circ$  step. T spectra at normal incidence (blue). (b) Dispersion under  $s$  (left) and  $p$  (right) polarizations, shown with circles and oblique squares. Blue dashed line is the dispersion evaluated from Eq. (1).

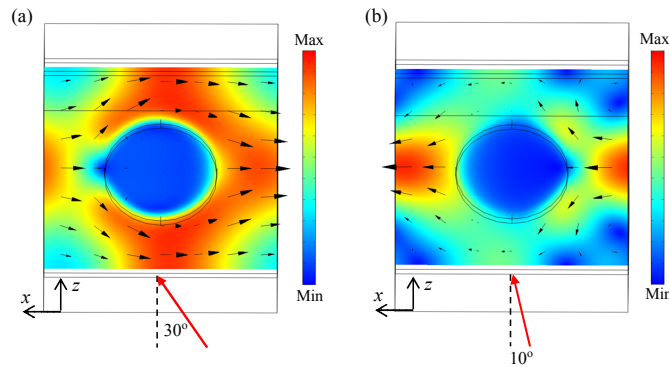


Fig. 3: In-plane time-averaged EM power flow of the lowest mode at (a) lower and (b) upper branches.

of light in vacuum. Equation (1) stems from a dispersion equation for a non-perforated MIM waveguide [7]. Here it is reduced in the first Brillouin zone and results in Eq. (1), which well reproduces the lower branch. Equation (1) means that the group velocity in plane is negative:  $d\omega/(dk) < 0$ .

Figure 3 shows in-plane time-averaged EM power flow (or Poynting flux) of the lowest mode: (a) the lower branch at 0.505 eV and  $30^\circ$  and (b) the upper branch at 0.620 eV and  $10^\circ$ . The unit cell in the  $xy$  plane is displayed (the  $y$  axis is set as shown in Fig. 1). Color plot shows the intensity and arrows denote three-dimensional vectors on the  $xy$  section in  $\text{Al}_2\text{O}_3$  layer with air hole. The Poynting flux was evaluated by finite element method (COMSOL Multiphysics). Obviously, negative Poynting flux for the  $x$ -component of incident wave vector is realised only at the lower branch [Fig. 3(a)].

#### 4. Conclusions

A typical fishnet MM has been analysed as a perforated MIM waveguide. It is directly shown that the lower branch of the lowest mode has in-plane negative Poynting flux. The negative group velocity is also derived from the dispersion equation. Negative refraction effect [8] comes from the feature of the eigenmode. The present analysis also implies the potential to realise negative refractive media at the longer wavelength ranges, based on MIM waveguides.

This study was partially supported by JST PRESTO program, by Cyberscience Center, Tohoku University, Japan, and by KAKENHI (Grant No. 22760047, 22109007) from JSPS and MEXT.

#### References

- [1] S. Zhang, W. Fan, N.C. Panoiu, K.J. Malloy, R.M. Osgood, and S.R.J. Brueck, Experimental demonstration of near-infrared negative-index metamaterials, *Phys. Rev. Lett.*, vol. 95, p. 137404, 2005.
- [2] M. Iwanaga, Subwavelength electromagnetic dynamics in stacked complementary plasmonic crystal slabs, *Opt. Express*, vol. 18, pp. 15389-15398, 2010.
- [3] M. Iwanaga, Electromagnetic eigenmodes in a stacked complementary plasmonic crystal slab, *Phys. Rev. B*, vol. 82, p. 155402, 2010.
- [4] L. Li, New formulation of the Fourier modal method for crossed surface-relief gratings, *J. Opt. Soc. Am. A*, vol. 14, pp. 2758-2767, 1997.
- [5] L. Li, Formulation and comparison of two recursive matrix algorithm for modeling layered diffraction gratings, *J. Opt. Soc. Am. A*, vol. 13, pp. 1024-1035, 1996.
- [6] A.D. Rakić, A.B. Djurušić, J.M. Elazar, and M.L. Majewski, Optical properties of metallic films for vertical-cavity optoelectronic devices, *Appl. Opt.*, vol. 37, pp. 5271-5283 (1998).
- [7] E.N. Economou, Surface plasmons in thin films, *Phys. Rev.*, vol. 182, pp. 539-554, 1969.
- [8] J. Valentine, S. Zhang, T. Zentgraf, E. Ulin-Avila, D.A. Genov, G. Bartal, and X. Zhang, Three-dimensional optical metamaterial with a negative refractive index, *Nature*, vol. 455, pp. 376-379, 2008.